IOPscience iopscience.iop.org

Home Search Collections Journals About Contact us My IOPscience

Aluminium valence and core excitonic states in GaAs-$Ga_{0.7}Al_{0.3}As$ systems

This article has been downloaded from IOPscience. Please scroll down to see the full text article.

1993 J. Phys.: Condens. Matter 5 1691

(http://iopscience.iop.org/0953-8984/5/11/009)

View the table of contents for this issue, or go to the journal homepage for more

Download details:
IP Address: 171.66.16.159
The article was downloaded on 12/05/2010 at 13:03

Please note that terms and conditions apply.

J. Phys.: Condens. Matter 5 (1993) 1691–1700. Printed in the UK

Aluminium valence and core excitonic states in GaAs–$Ga_{0.7}Al_{0.3}As$ systems

F Vergand†, P Jonnard†, M Kefi†, C Bonnelle†, C Deparis‡ and J Massies‡

† Laboratoire de Chimie Physique Matière et Rayonnement, Université Pierre et Marie Curie, Unité associée au CNRS 176, 11 rue Pierre et Marie Curie, 75231 Paris Cédex 05, France

‡ Laboratoire de Physique du Solide et Energie Solaire, CNRS–Sophia Antipolis, 06560 Valbonne, France

Received 9 November 1992, in final form 21 December 1992

Abstract. The Al 3p occupied density of states in GaAs(30 Å)–$Ga_{0.7}Al_{0.3}As$(31 Å) heterostructures is studied and compared with that of bulk $Ga_{0.7}Al_{0.3}As$ through x-ray emission spectroscopy induced by electrons. The radiative recombination of the Al 1s core exciton is also analysed. Partial dehybridization of the Al p and s valence and conduction states is observed for the first time in the barriers of a superlattice and of a single quantum well. These changes suggest that the Al electron distributions of neighbouring barriers are not coupled in heterostructures of 30 Å period and are governed by their quasi-2D character.

1. Introduction

The GaAs–$Ga_{0.7}Al_{0.3}As$ heterostructures have been the object of extensive investigation because these systems have properties of great practical and theoretical interest [1, 2]. The optical properties of superlattices have been widely studied [3, 4] in order to determine the influence of their quasi-two-dimensional structure on the electron and hole states. For superlattices with larger periods (greater than 60 Å), it has been found that the motion of the electrons and holes *at the band edge* is quantized in the growth direction while along the layers the motion has a two-dimensional (2D) character. As the superlattice period is reduced to a few monolayers, the electrons and the holes are no longer bound and their distribution loses its 2D character [5–8].

For a full understanding of these systems, the densities of states (DOSs) must be known *in the total energy range of the valence band*. We report the Al 3p valence DOS of $Ga_{0.7}Al_{0.3}As$ in the barriers of a GaAs(30 Å)–$Ga_{0.7}Al_{0.3}As$(31 Å) superlattice and of a single quantum well compared with those of the bulk ternary compound and at the GaAs–$Ga_{0.7}Al_{0.3}As$ interface.

The Al 3p DOS is obtained from the Al 3p–1s dipolar radiative transition using electron-induced x-ray emission spectrometry (EXES) [9]. Bulk materials as well as layered systems and interfaces can be analysed by this method. Radiative recombination of the Al 1s core exciton can also take place [10] and the binding energy, intensity and width of the excitonic state can be deduced by EXES for the various materials.

0953-8984/93/111691+10$07.50 © 1993 IOP Publishing Ltd

In section 2 we describe the preparation of the samples and we recall the principle of EXES and the experimental conditions which allow its application to the study of bulk materials, interfaces or layered systems. In section 3 we present the EXES spectra of the various systems and we discuss them in comparison with experimental data obtained previously on the Al 3p valence states of bulk AlAs and GaAs–AlAs interface and with the experimental data taken from the literature. In section 4 we report the core excitonic emissions. Concluding remarks are given in section 5.

2. Samples and method of analysis

2.1. Sample preparation and characterization

Three samples labelled B, SL and QW were prepared using molecular beam epitaxy. The samples were grown on a GaAs buffer layer 1 μm thick deposited on GaAs(100) substrates doped with 10^{18} Si cm^{-3}; the samples were protected with a GaAs layer 100 Å thick. Sample B is bulk $Ga_{0.7}Al_{0.3}As$ 1500 Å thick. Sample SL is a superlattice consisting of 24 periods of $Ga_{0.7}Al_{0.3}As$(31 Å)/GaAs(30 Å). Sample QW is a single quantum well 30 Å thick surrounded by two $Ga_{0.7}Al_{0.3}As$ barriers 31 Å thick. The deposition rates are 0.35 μm h^{-1} for GaAs and 0.5 μm h^{-1} for $Ga_{0.7}Al_{0.3}As$; the substrate temperatures of 600 °C were the same for the three samples. Rotation of the substrate during deposition ensured good homogeneity of the compounds. To obtain heterostructures of good structural quality, the growth was interrupted at the end of each layer deposition. RHEED oscillation patterns [11] and photoluminescence spectra involving the valence excitonic level [12] were analysed for samples SL and QW and showed a low roughness of layers and a very few defects.

2.2. Method of analysis

By means of an electron beam, Al 1s core holes are created in the samples. The 3p–1s radiative recombination is then analysed with the aid of a bent-crystal x-ray vacuum spectrometer of the Johann type. The bent crystal is a quartz blade with $10\bar{1}0$ planes parallel to the curved faces. The detector is a gas flow counter (90% Ar–10% CH_4) working in the Geiger–Müller region. The spectral resolution is about 2×10^{-4} and the photon energy is determined to within about ± 0.2 eV.

The energy of the incident electrons is an important parameter. Indeed, for photons and electrons of equivalent energy, the photon escape depth is greater than the electron excitation depth. Then, the analysed sample depth is determined by the energy E_0 of the incident electron beam. As is well known, electrons lose energy by going through a material. Using this property and the fact that only electrons having an energy higher than the Al 1s ionization energy (1560 eV) are efficient, we adjust the energy E_0 of the incident electrons so that a well defined thickness in the sample can be analysed. The orders of magnitude of the mean energies of electrons inside the material can be deduced from one of the empirical relations [13] between the practical range R (Å) of the electrons and the energy E:

$$R\ (\text{Å}) = (900/\rho^{0.8}) E\ (\text{keV})^{1.3}$$

where ρ (g cm^{-3}) is the specific gravity. On increasing E_0 the analysed thickness and the number of emitted photons increase.

To study bulk $Ga_{0.7}Al_{0.3}As$ (sample B), we have chosen an incident energy equal to 4300 eV; we estimated that the energy of electrons is about 4000 eV at the surface of $Ga_{0.7}Al_{0.3}As$; then the emissive thickness (where electrons have an energy larger than the 1s ionization energy) is about 1100 Å, i.e. the major part of the sample.

To study the $Ga_{0.7}Al_{0.3}As$–GaAs interface, we used the interfacial region of sample B between the top layer and the bulk ternary compound. The method is the same as that employed for numerous other solid–solid interfaces [14]. In this method, the incident energy is such that, after the electrons have gone through the GaAs upper layer, their mean energy E must be just superior to the threshold ionization energy of the analysed line. The closer E is to the threshold energy, the thinner the analysed thickness at interface. Indeed, the electrons present a distribution in energy. The shape of this distribution depends on the ratio x/R, where x is the length of the path in the upper layer. We measured the number of emitted Al 3p → 1s photons in the range from $E_0 = 1500$ eV to $E_0 = 2300$ eV and plotted it versus E_0. We obtained a threshold at about 1700 eV. The difference between this value and the Al 1s energy (1560 eV) results from the energy losses in GaAs. We obtained a spectrum for the interface with $E_0 = 2050$ eV which was the lower limit for a reasonable but poor counting rate. From Fitting's results we estimated that the mean energy of electrons on the $Ga_{0.7}Al_{0.3}As$ surface is about 1900 ± 100 eV, i.e. about 340 eV higher than the Al 1s threshold energy. Using the data concerning electron paths and their energy losses [15], we estimated that the analysed thickness is less than 100 Å at the interface.

To study the superlattice we used an energy $E_0 = 5000$ eV so as to analyse the whole sample; this energy has been determined as previously. For the barriers of the single quantum well we chose an energy $E_0 = 3500$ eV in order to obtain an appreciable value of the ionization cross section; indeed the ionization cross section becomes the main parameter for determining the intensity in this case when the amount of emissive Al atoms is low, i.e. about 1.4×10^{15} atoms.

The intensity of an x-ray emission describes the energy distribution of the final state; it depends on the transition matrix element, i.e. here on the amplitude of the Al 3p wavefunction in the region of the 1s highly localized core hole. For the Al 3p → 1s transition in III–V semiconductors, a one-electron model is known to be sufficient [10]. Then, if the radiative transition probability is constant along the emission band, the spectral density describes the k-space integrated distribution of a hole in the local and partial valence DOSs *around aluminium atoms*. A spectral change characterizes a change in the DOS in the ground state.

3. Al 3p valence states

No emission line of Ga and As is present in the Al 1s range. The quasi-linear background due to bremsstrahlung has been subtracted from the spectra. The curves represent normalized intensity versus photon energy. For comparison with spectra in other energy ranges, the curves are adjusted relative to the top E_V of the valence band, which is determined by extrapolating the linear part of the high-energy side of the emission. The bottom E_C of the conduction band is located at a distance equal to the gap width at room temperature (1.85 eV [16]). Above E_V, the counting time is ten times that for the valence band.

3.1. Bulk $Ga_{0.7}Al_{0.3}As$

Figure 1(*a*) shows the Al 3p → 1s emission of sample B (full circles). It presents a non-structured main peak and a wide shoulder lying between about 4.7 and 8.5 eV; another shoulder with a lower intensity widens the emission down to 12.8 eV. A faint structure is observed in the gap at 0.25 eV below E_C; it will be discussed in the next section. We compare the Al 3p → 1s emission of bulk $Ga_{0.7}Al_{0.3}As$ with the AlAs emission [10] (broken (short dashes) curve in figure 1(*a*)). The main peak and the lower shoulder are almost similar. The first shoulder is slightly shifted towards higher binding energies in the ternary. Both this shoulder and the main peak are broadened.

For $Ga_{0.7}Al_{0.3}As$, as for AlAs, hybridization of the valence states is present for the whole band spread. This is seen by considering the Al 3s → 2p and As 4p → 3d emissions of $Ga_{0.7}Al_{0.3}As$ [17, 18] (figure 1(*b*)). In the range of the main peak, the Al 3p states are predominant relative to the Al 3s states, while in the range of the first shoulder the Al 3p states are strongly mixed with Al 3s states. The energy and the shape of the Al 3p and As 4p peaks are very similar, showing that these two distributions are strongly mixed. The lower shoulder comes from a mixing between Al 3p, Al 3s and As 4s states. A mixing of the Al and Ga DOSs must also be present in the ternary. Because in the binaries these DOSs are similar but slightly shifted [19, 20], a broadening is foreseen for the ternary spectral DOS, in agreement with our observations. Such broadening has also been seen using UPS and ascribed to an alloying effect [21]. Owing to anion disorder in the alloy, it has been shown that E_V shifts towards a higher photon energy with decreasing x in $Ga_{1-x}Al_xAs$ [18]. An increase of 0.15 eV has been found between $x = 1$ and $x = 0.3$ from the Al $L_{2,3}$ (3s → 2p) emission. By decomposing our experimental spectrum as described in section 4, we determine an increase of 0.2 eV between AlAs and $Ga_{0.7}Al_{0.3}As$ in good agreement with the cited reference. So the differences between the spectra of AlAs and $Al_{0.3}Ga_{0.7}As$ can be interpreted as due to alloy disorder.

In figure 1(*c*) we present the total spectral density of $Ga_{0.6}Al_{0.4}As$ as obtained by XPS [22]. The composition of the material is slightly different from ours but the expected energy shifts are sufficiently small that the spectra could be compared. Indeed the XPS spectrum and the EXES spectra show rather good agreement for the positions of the experimental peaks especially for the first peak and the energy E_V. Note that the spectral intensities cannot be compared because EXES gives the local and partial DOSs while XPS involves the total DOSs weighted by photoabsorption cross sections.

To our knowledge no partial p cation DOS has been calculated for III–V ternary compounds but they are assumed to be close to those for binary compounds. GaAs can be considered as representative of III–V compounds, a slight shift and broadening being expected depending on the nature of the cations. We plot in figure 2 the partial p cation DOS calculated for GaAs [23] from a tight-binding (TB) Hamiltonian. This Hamiltonian has been constructed by a least-squares fit to an empirical pseudopotential calculation [24]. It contains the s and p orbitals of both Ga and As; it is orthogonal and is based on 22 TB parameters in the two-centre approximation. The calculated DOS has been broadened by a Lorentzian curve of full width at half-maximum (FWHM) $L_{1/2}$ equal to 0.6 eV. Agreement between the experimental and calculated curves is rather good except for the intensity of the 6 eV shoulder which is higher for the calculated DOS than for the spectral density. This is probably due to the matrix element which is not included in the calculations. Indeed

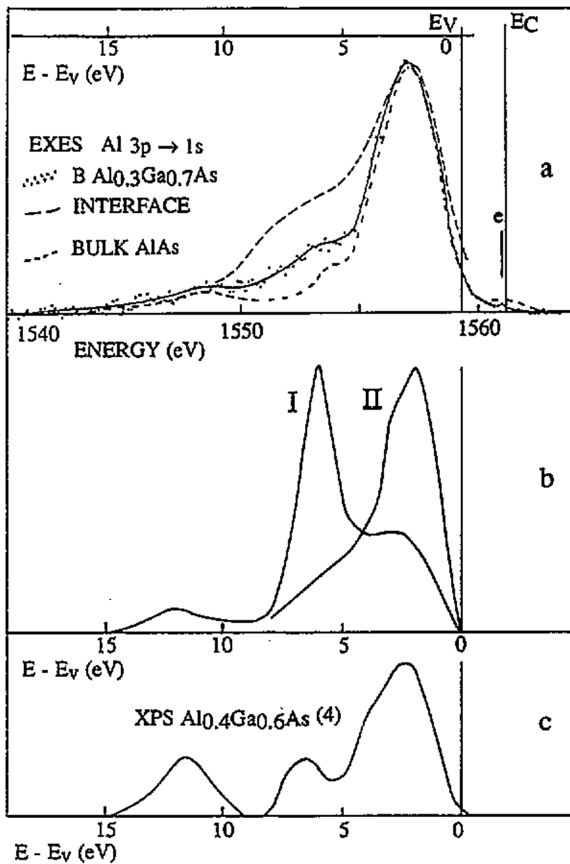

Figure 1. (*a*) Al 3p → 1s and Al 1s core exciton e in bulk $Ga_{0.7}Al_{0.3}As$ (sample B) (—●—), Al 3p → 1s emission in bulk AlAs [10] (----) and Al 3p → 1s emission at the GaAs–$Ga_{0.7}Al_{0.3}As$ interface (– – –). (*b*) Al 3s → 2p (curve I) (photon energy range, about 70 eV) and As 4p → 3d (curve II) (photon energy range, about 40 eV) in bulk $Ga_{0.7}Al_{0.3}As$ [17]. (*c*) XPS valence band in bulk $Al_{0.4}Ga_{0.6}As$ [22].

the matrix elements of the radiative transition between a core level and quasi-pure p or highly hybridized p–s states are expected to be different; the more extended the valence states are, the smaller is the matrix element. Then, the intensity ratio of the first shoulder on the main peak is expected to be lower for the spectral density than for the calculated DOS.

3.2. GaAs–$Ga_{0.7}Al_{0.3}As$ interface

The interface spectrum is shown in figure 1(*a*) (broken (long dashes) curve) together with the bulk spectrum (full circles). As already emphasized, the emissive thickness was less than 100 Å. The most efficient region is that closest to the interface because the number of effective electrons rapidly decreases with increasing depth. Consequently the number of atoms which participate in the spectrum is small and the interface spectrum presents poor statistics. The main peak is similar to that of the bulk but a clear increase in the spectral Al 3p DOS is observed in the range of

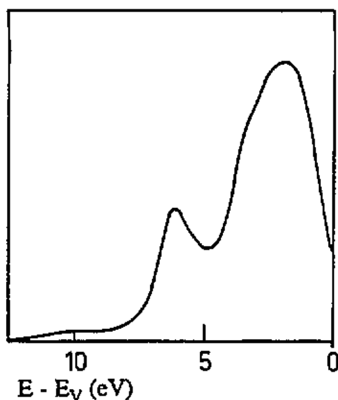

Figure 2. Calculated partial p and local Ga DOS in GaAs.

the Al 3p → Al 3s mixed states (first shoulder); this result resembles what we have observed for the GaAs–AlAs interface [25].

Baldereschi *et al* [26] have estimated the effect of compositional and positional (local lattice distortion) disorders in $Al_xGa_{1-x}As$. They were interested in the energy gap and their results for valence states concern only the first 5 or 6 eV from E_V, i.e. the range of the main peak. Because the difference between the electronegativities of Al and Ga is small and because GaAs and AlAs have nearly the same lattice constants, they found that chemical and positional disorder should have rather a limited effect on the main peak. This agrees with our observation. On the contrary, in the energy range of the first shoulder, broadening is foreseen at the GaAs–$Ga_{1-x}Al_xAs$ interfaces when the states of the two materials are mixed [19] and defects such as wrong cation–cation bonds are present [27]. Because a large broadening is observed, one expects these types of defect to be present at the interface studied here.

3.3. *Superlattice and single quantum well*

Figure 3 shows the Al 3p → 1s emission of the sample SL (full circles) together with the bulk ternary spectrum (full curve). The three typical parts of III–V compound spectra are present and also a faint structure, located at 0.7 eV below E_C, which will be discussed in section 4 together with that in bulk. The main peak and the lower shoulder are superimposable on those of the bulk. A strong change in the spectral density is seen in the range of the first shoulder where we observe a small and well resolved feature located 5.8 eV below E_V. A similar result is obtained for sample QW. The spectrum for sample SL has a shape analogous to the bulk AlAs spectrum but the energy of the feature in the spectrum of sample SL does not coincide with the first shoulder of AlAs, showing that the two systems are different. Changes in the DOS induced by variations in atomic arrangement, defects [25], etc, are located in this energy range but, as seen in the interface spectrum, they introduce a broadening of features and not a well resolved structure.

This structure in the spectrum for sample SL is in an energy range where the Al 3p states are mixed with predominant Al 3s states. Its presence suggests that Al p states are less hybridized and less extended in the layered samples. Thus, the layered structure induces partial localization of the states which are the most hybridized with extended s states in the 3D bulk material.

Calculations made within the framework of the local-density-functional theory, by means of the self-consistent relativistic linear muffin-tin orbital method, for

$[(GaAs)_2-(AlAs)_2]$ superlattices have shown that reduced periodicity in the [001] growth direction leads to a low dispersion of the states at the bottom of the upper part of the valence band, about 5.8 eV below E_V, because of the reduction in the Brillouin-zone size [28]. This range corresponds to that of the well resolved structure which we observed in the EXES spectrum. However, it must be emphasized that these theoretical results concern ultra-thin superlattices. For the period considered here, the effect of the Brillouin-zone size must be very small. In fact, we obtain the same results for sample SL as for sample QW where no periodicity is present.

Thus we suggest that dehybridization of states, as seen for the first time in our EXES spectra, is due to the 2D character of the structure of the barriers. From our results a net decrease in valence electronic coupling exists between 30 Å neighbouring barriers.

4. Al 1s transitions from gap states

We consider here the faint structures observed in the band gap for the bulk and for sample SL. We cannot discuss the data for sample QW and the GaAs–$Ga_{0.7}Al_{0.3}As$ interface, because of their poorer statistics. As seen for AlAs [10] and other semiconductors [29, 30], an emission from a level located in the band gap can be interpreted as the radiative recombination of a core excitonic state created simultaneously with the core hole. For core excitons, the electron–hole interaction is dominant and the exciton radius is known to be only a few angströms.

To determine the characteristics of the excitonic Al 1s transitions, we have first decomposed the bulk spectrum in the region 1555–1565 eV (figure 4(*a*)). The valence band edge is fitted by a linear law as usual in high-energy spectroscopies $(E - E_V)$; this function is broadened by convoluting it with a Lorentzian curve of FWHM $L_{1/2}$ equal to 0.6 eV, which takes into account the broadening due to the known Al 1s core hole lifetime (about 10^{-15} s) and the instrumental window. The excitonic transition is centred at the experimental energy E_e. It is fitted by convoluting a Lorentzian curve with a Gaussian curve of FWHM $G_{1/2}$. Because the broadening due to the phonon lifetime is relatively small, the Gaussian involves essentially the structural disorder of the bulk ternary compound. A good fit is obtained with the same Lorentzian curve for the valence band and the excitonic emission; this supposes that the lifetimes of the bare core hole and of the excitonic state are the same. The decomposition parameters are plotted in table 1.

Table 1. Energy E_V of the top of the valence band and characteristics of the excitons, namely E_e, E_b, $L_{1/2}$, $G_{1/2}$ and I_e which are the position, binding energy, Lorentzian width, Gaussian width and the intensity, respectively. The error in the energy is ±0.2 eV.

Sample	E_V (eV)	E_e (eV)	E_b (eV)	$G_{1/2}$ (eV)	$L_{1/2}$ (eV)	I_e
B	1559.5	1561.1	0.25	0.6	0.6	0.004
SL	1559.6	1560.8	0.65	0.6	1.2	0.026

For sample SL (figure 4(*b*)) the binding energy, intensity and width of the observed transition are clearly larger than for the bulk. A good fit is obtained with the same value of $G_{1/2}$ and a value of $L_{1/2}$ broader for sample SL than for sample B (table 1).

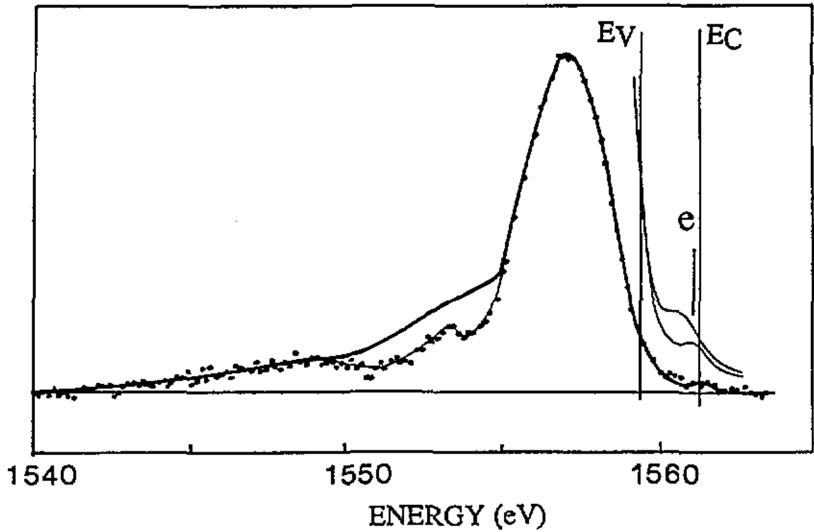

Figure 3. Al 3p → 1s and Al 1s core exciton in a GaAs–$Ga_{0.7}Al_{0.3}As$ superlattice (sample SL) (—●—), and Al 3p → 1s in sample B (——). For the Al 1s core exciton e, the calculated curves for sample SL (upper curve) and for sample B (lower curve) (——) are also shown.

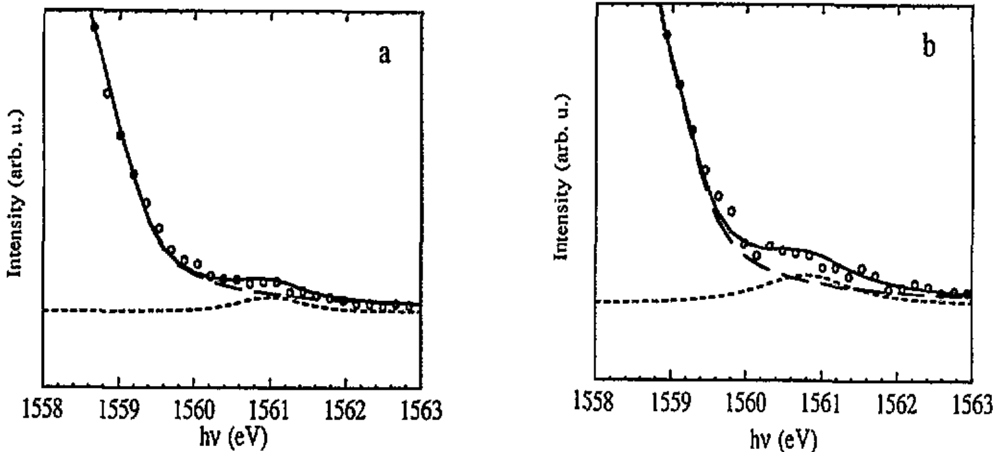

Figure 4. Decomposition of the Al 3p → 1s edge and the Al 1s core exciton e (*a*) in bulk $Ga_{0.7}Al_{0.3}As$ and (*b*) in a GaAs–$Ga_{0.7}Al_{0.3}As$ superlattice: —○—, experiment; — — —, valence band edge; - - - -, exciton.

Thus the excitonic state lifetime of sample SL should be shorter than that for the bulk. This is consistent with the variation in exciton characteristics and should indicate that the radius of the exciton decreases for sample SL [31], making the localization of the excitonic state increase strongly. Simultaneously with the localization, dehybridization of Al states should be present in this range of the conduction band for sample SL. However, it must be emphasized that the interface state can also be present. The

observed changes should be due to the simultaneous presence of several unresolved transitions from interface and excitonic states.

For the bulk ternary compound, the radiative recombination of the Al 2p exciton state has been observed [29]. Its FWHM is 0.6–0.8 eV. The lifetime of the Al 2p core hole is about ten times that of the Al 1s core hole. The Lorentzian broadening can thus be neglected and the emission is characterized by a Gaussian curve whose width is in good agreement with our value of $G_{1/2}$. The excitonic 2p level is located above the bottom of the conduction band. Indeed, states of different symmetries are concerned; the 2p exciton line involves s conduction states while we probe p states. Our results show that states present at the bottom of the conduction band have a p character.

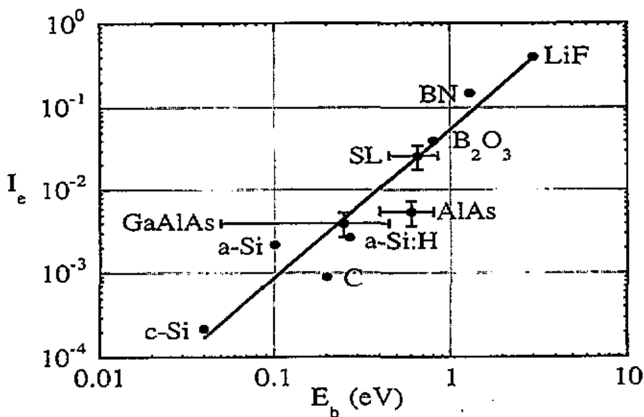

Figure 5. Log–log plot of 1s and 2p exciton intensity versus their binding energy for AlAs, $Ga_{0.7}Al_{0.3}As$ and the GaAs–$Ga_{0.7}Al_{0.3}As$ superlattice (sample SL) (this work and [10]) and for other materials [30].

We show in figure 5 a log–log plot of 1s and 2p core exciton intensity I_e versus the binding energy E_b for seven materials [30]. It appears that the data can be fitted by a power law and the intensity varies as the square of the binding energy. We have indicated on the same plot our data for bulk AlAs and $Ga_{0.7}Al_{0.3}As$ in samples B and SL. When our error bars are taken into account, our values are in good agreement with the previous fit. This suggests that the structure that we observe is an excitonic transition rather than recombination from interface states.

5. Conclusion

The present study describes the changes in the Al 3p partial DOS in heterostructures. The partial dehybridization observed for Al p and s valence and conduction states in samples SL and QW shows that the DOSs are strongly influenced by the 2D character of the structure at energies far from the band edges. These changes affect essentially the states of s character or those mixed with them because they are the more diffuse band states, i.e. the more sensitive to the atomic environment. Therefore,

the neighbouring barriers are not electronically coupled in heterostructures of 30 Å period and it is no longer possible to treat each layer as bulk-like material. EXES has proved its usefulness as a local and partial-DOS analysis method of semiconductor heterostructures in energy and depth ranges which are not easily accessible by other spectroscopies but are important for a full understanding of these materials.

Acknowledgments

The authors are grateful to Dr D A Papaconstantopoulos for providing the theoretical DOSS and for helpful discussions. The work has been partially supported by the EEC through contract ST2J-254.

References

[1] Adachi S 1985 *J. Appl. Phys.* **58** R16
[2] Bastard G 1988 *Wave Mechanics Applied to Semiconductor Heterostructures* (Paris: Les Editions de Physique)
[3] Cingolani R, Ferrara M, Lugara M, Moro C, Chen Y, Bassani F, Massies J and Turco F 1988 *Europhys. Lett.* **7** 651
[4] Cingolani R, Chen Y and Ploog K 1989 *Superlatt. Microstruct.* **5** 359
[5] Chomette A, Lambert B, Deveaud B, Clerot F, Regreny A and Bastard G 1987 *Europhys. Lett.* **4** 461
[6] Cingolani R, Baldassarre L, Ferrara M, Lugara M and Ploog K 1989 *Phys. Rev.* B **40** 6101
[7] Gopalan S, Christensen N E and Cardona M 1989 *Phys. Rev.* B **39** 5165
[8] D'Andrea A, Del Sole R and Cho K 1990 *Europhys. Lett.* **11** 169
[9] Bonnelle C 1987 *Royal Society of Chemistry Annual Report* C p 201
[10] Vergand F, Jonnard P and Bonnelle C 1989 *Europhys. Lett.* **10** 67
[11] Massies J 1988 *Les Interfaces et la Liaison Chimique* (Paris: Les Editions de Physique) p 15
[12] Deparis C, Massies J and Neu G 1990 *Appl. Phys. Lett.* **56** 233
[13] Fitting H J 1974 *Phys. Status Solidi* a **26** 525
[14] Bonnelle C and Vergand F 1989 *J. Chim. Phys.* **86** 1293, and references therein
[15] Ashley J C, Tung C J, Ritchie R H and Anderson V E 1976 *IEEE Trans. Nucl. Sci.* **NS-23** 1833
[16] Bosio C, Stahli J L, Guzzi M, Buri G and Logan R A 1988 *Phys. Rev.* B **38** 3263
[17] Terekhov V A, Khashkharov V M, Domashevskaya E P, Arsent'ev N N and Ivanova I M 1989 *Sov. Phys.–Semicond.* **23** 167
[18] Tsang K L, Rowe J E, Calcott T A and Logan R A 1988 *Phys. Rev.* B **38** 13277
[19] Min B I, Massida S and Freeman A J 1988 *Phys. Rev.* B **38** 1970
[20] Magri R, Froyen S and Zunger A 1991 *Phys. Rev.* B **44** 7947
[21] Okumura H, Yoshida I, Misawa S and Yoshida S 1987 *J. Vac. Sci. Technol.* B **5** 1622
[22] Ludeke R, Ley L and Ploog K 1978 *Solid State Commun.* **28** 57
[23] Papaconstantopoulos D 1992 private communication
[24] Chelikowsky J R and Cohen M L 1976 *Phys. Rev.* B **14** 556
[25] Jonnard P, Vergand F, Bonnelle C, Deparis C and Massies J 1991 *J. Phys.: Condens. Matter* **3** 3433
[26] Baldereschi A, Hess E, Maschke K, Neumann H, Schulze K R and Unger K 1977 *J. Phys. C: Solid State Phys.* **10** 4709
[27] O'Reilly E P and Robertson J 1986 *Phys. Rev.* B **34** 8684
[28] Cai Y Q, Riley J D, Leckey R C G, Usher B, Fraxedas J and Ley L 1991 *Phys. Rev.* B **44** 3787
[29] Carson R D and Schnatterly S E 1987 *Phys. Rev. Lett.* **59** 319
[30] Nithianandam J and Schnatterly S E 1990 *Phys. Rev.* B **42** 3038
[31] Strinati G 1984 *Phys. Rev.* B **29** 5718